An Adaptive General Type-2 Fuzzy Logic Approach for Psychophysiological State Modelling in Real-Time Human-Machine Interfaces

Changjiang He, Mahdi Mahfouf, and Luis A. Torres-Salomao, *Member IEEE*

***Abstract*—In this research paper, a new type-2 fuzzy-based modelling approach is proposed to assess human operators' psychophysiological states for both safety and reliability of human-machine interface systems. Such a new modelling technique combines type-2 fuzzy sets with state tracking to update the rule base through a Bayesian process. These new configurations successfully lead to an adaptive, robust and transparent computational framework that can be utilised to identify dynamic (i.e., real time) features without prior training. The proposed framework was validated on mental arithmetic cognitive real-time experiments with ten (10) participants. It was found that the proposed framework outperforms other paradigms (i.e., an adaptive neuro-fuzzy inference system and an adaptive general type-2 fuzzy c-means modelling approach), in terms of disturbance rejection and learning capabilities. The proposed framework achieved the best performance compared to other models that have been presented in the related literature. Therefore, the new framework can be a promising development in human-machine interface systems. It can be further utilised to (i) develop advanced control mechanisms, (ii) investigate the origins of human compromised task performance and (iii) identify and remedy psychophysiological breakdown in the early stages.**

***Index Terms*—Human-machine interface, type 2 fuzzy sets, psychophysiology, modelling, real time, adaptive.**

I. Introduction

TODAY'S automatic systems have been widely implemented in diverse areas, from daily life to global regulations. The combination of an automatic system and a human operator can have several advantages, including fast reaction to and processing of a large amount of concurrent information [1]. Due to this revolutionary intelligent power, automatic systems are currently commonly adapted in many important management and operation systems , such as manufacturing, transportation and clinical medicine [2], [3].

There are, however, many barriers yet to be broken for such a combination to fulfil its full potential advantages and reach its theoretical efficiency. The lack of trust and over-trust with high expectations towards automatic systems have compromised the overall performance of this combination, whereas the increases in operational demands of human operators threaten the reliability and safety of the whole system [1], [2]. Therefore, it is of paramount importance to introduce a mechanism that can bridge the communication gap between the automatic system and the so-called 'human in the loop'.

Humans respond to environmental stimuli through conditioned reflex and subject to personal experience and psychophysiological state [4]. human-machine interface (HMI) consists of communications at three different levels, direct technical, emotional and mental. Collaboration at different levels and diverse dynamic individual states lead, as a result, to networks with high complexity and uncertainty [1]. This requires a shift from traditional modelling approaches primarily depending on mathematical expressions and physical laws towards data-driven modelling approaches led by powerful pattern recognition of fast data mining. These techniques, such as artificial neural networks and fuzzy logic systems, exhibit an extraordinary ability to generate and apply conditional patterns under uncertain environments with limited quantities of data.

For the safety of HMI systems, the critical thinking and reasoning of human operators should always be an intrinsic part of the final decision and cannot be fully replaced by automation. The decision of splitting the workload into automatic systems and human operators leads to human-centred modelling to estimate the operator's psych-physiological state [2], [5]–[19]. The existing approaches for predicting the human psychophysiological state within HMI systems mainly rely on data-driven methods. The commonly used frameworks include the adaptive neuro-fuzzy inference system (ANFIS), type-1 Mamdani fuzzy model, proportional integral Mamdani fuzzy model, type-2 fuzzy model and support vector machines (SVMs). The majority of the presented models have fixed configurations based on off-line training sessions. This model structure limits the models to those who share similar patterns to the training samples. As a result, the prediction accuracy continuously decreases with time due to a lack of flexibility. Therefore, self-organising and adaptive learning have been explored in some newly developed modelling approaches of this research area (e.g., the A-GT2-FCM framework [16]).

However, the nonlinear changes in psychophysiological state and the lack of flexible weight adjustment for inter- and intra-uncertainty compromise the accuracy performance of these models. Failures are commonly associated with extreme psychophysiological states such as breakdown, multitasking and fatigue; model performance is either compromised or severely lagging because of them. It is worth noting that current frameworks and models [5]–[19] cannot fulfil one or more of the following essential requirements for HMI systems:

1) Adaptability: the ability to reconfigure themselves con-

C. He and M. Mahfouf are with the Department of Automatic Control and Systems Engineering, The University of Sheffield, Sheffield, S1 3DJ, UK, e-mail: che5@sheffield.ac.uk; m.mahfouf@sheffield.ac.uk.

L. A. Torres-Salomao is with Digital Unit, Kellogg Latin America, Queretaro, Mexico, e-mail: latsalomao@ieee.org.

Manuscript received ... .., ...; revised ... .., ...

sistently according to real-time system changes.

2) Intelligence: specifically refers to the ability to interpret the system state and modify its inference engine correspondingly.
3) Robustness: the ability to handle inter- and intra-uncertainty and being generalised to any human operator.
4) Being Explicit: the ability to summarise the learning experiences via easy to understand logical statements.

It is important to address the abovementioned features in predicting the human operator psychophysiological state. To balance the HMI system, a more sophisticated model using easy-to-access psychophysiological data in addition to existing models and frameworks is required.

This paper is organised as follows: Section II introduces the HMI system simulation, explains the experimental configurations and presents the selection of psychophysiological biomarkers applied in this research. A new adaptive general type-2 fuzzy modelling system is proposed in Section III. The comparison of experimental results with other models is provided in Sections IV. The last section concludes this study and suggests future areas of the research.

II. Human-Machine Interface Experiment

A. Human-Machine Interface Simulation

The priority of the human-machine interface (HMI) simulation experiment is to challenge the participants' problem-solving ability in a similar manner to real-world HMI situations. In contrast to human-human interfaces, human participants from the HMI demonstrate lower emotional intensity over less diverse feelings [1], [20]. Therefore, the simulation should be able to introduce adequate adjustable stimuli. Various observable psychophysiological alterations triggered by these stimuli should resemble those in real-life situations [1]. The most frequently used HMI simulations in the field of published research are Stroop colour-word interference, mental arithmetic and virtual vehicle operation [16], [21]–[26]. In this research, mental arithmetic has been selected as the HMI simulation for the following reasons:

1) Effectiveness: Compared to mental arithmetic, the psychophysiological changes triggered by the stimuli of Stroop colour-word interference are less significant and influenced by inherent human body regulation [21]–[24]. Additionally, different from the mental arithmetic, the simulation environment and the maintenance of the virtual vehicle operation can significantly influence the system effectiveness [27], [28].
2) Simplicity: Unlike mental arithmetic, the use and reproductivity of virtual vehicle operation can be compromised by its cost and complexity [25], [26].
3) Intuitiveness: Mental arithmetic only requires basic knowledge of arithmetic regardless of the most inter- and intra-individual differences.

B. Data Acquisition

The data of the selected psychophysiological biomarkers for this experiment are collected from four major measurements: electroencephalogram (EEG), electrocardiogram (ECG), pupil sizes and facial temperatures. EEG and ECG are recorded by the Biosemi®ActiveTwo system with a sampling frequency of 2,048 Hz. EEG signals are collected from the 32-channel system according to the standard Biosemi 10/20 layout. ECG signals are collected from the triangle 3-lead system covering the heart area. The initial filtering and reconstruction of signals are processed by Biosemi®ActiView software. Pupil movements are monitored with a Gazepoint eye-tracking camera, and the sizes are calculated by the Gazepoint software. Facial temperatures are based on infrared imaging recordings from an FLIR E40bx thermal imaging camera at a sampling frequency of 10 Hz. The data recording methods follow the experimental frameworks in [12], [14]–[16], [29], [30].

The mental arithmetic applied in this research is based on the MATLAB®GUI app similar to the app used in [15], [16], [29], [30]. The participants in this research are ten (10) healthy students from the University of Sheffield aged from 22 to 30. The selected subjects include both genders from different countries and backgrounds. The participants are advised to abstain from taking any medication, coffee or alcohol at least two hours before the experiment to avoid any bias in task performance and psychophysiological measurements.

C. Modelling Experiment Configuration

For the modelling configuration, the psychophysiological data are recorded from the participants during the premeditated HMI simulation sessions. The predictions of subjects' task performances are generated by the computational framework of the adaptive general type-2 fuzzy model based on the recordings in real time.

The whole prediction experiment for one subject lasts approximately 30 minutes, including two 12-minute mental arithmetic test sessions and a 5-minute break in the interval. The participants are required to complete a two-number multiplication within a certain amount of time in the mental arithmetic test. In each test session, there are four 3-minute phases with different difficulty levels. The first difficulty level requires the subjects to answer the multiplication questions of two random one-digit numbers within ten seconds. Compared with the first difficulty level, the second difficulty level only provides five seconds for each question. The third and fourth levels follow the same answering time pattern as the first and second levels except for switching the questions to the multiplication of a one-digit number and a two-digit number, both randomly generated. The order of the difficulty levels is different between two mental arithmetic sessions for checking the adaptiveness of the model, with incremental difficulty levels in the first session and randomised difficulty levels in the second session. The task performance is measured with the accuracy of 12 continuous operations.

D. Psychophysiological Biomarkers

The psychophysiological biomarkers applied for the model prediction are heart rate variables (HRV), task load indices (TLI), pupil diameter marker (PMD) and facial temperatures.

They are correspondingly based on ECG, EEG, eye-tracking camera and thermal camera measurements.

Heart rate variables are connected with the respiratory cycle, blood pressure and heartbeat fluctuation, which are under the control of the central nervous system [31]. The HRV indicators HRV_1 and HRV_2 in this research have already been used in previous experiments and studies of the University of Sheffield [9], [13]–[16], [30]. HRV_1 represents the 0.1 Hz component of the ECG signal, and it is measured by averaging the power spectrum of frequency components from $0.07\,\text{Hz}$–$0.14\,\text{Hz}$ in a time period of 30 seconds. HRV_2 is the ratio between the standard deviation and the mean value of the ECG signal in the same time frame.

Task load indices are designed as the measurements for the working memory, which corresponds to one's ability to maintain attention to a specific event while ignoring any other disturbance [5], [32], [33]. In this research, the two selected TLIs are TLI_1 and TLI_2, and they are calculated with the following equations:

$$
\begin{aligned}
TLI_1 &= \frac{P_{\theta,F_z}}{P_{\alpha,P_z}}, \\
TLI_2 &= \frac{P_{\theta,AF_z}}{P_{\alpha,CP_z,PO_z}},
\end{aligned}
\tag{1}
$$

where P_θ and P_α are the energy from the theta band $4\,\text{Hz}$–$7.5\,\text{Hz}$ and the alpha band $8\,\text{Hz}$–$12.5\,\text{Hz}$. The energy is measured by averaging the specific frequency range of the power spectrum over 30 seconds. The electrodes of F_z, P_z, AF_z and the combination of CP_z and PO_z follow the Biosemi 10/20 system [9], [13]–[16], [30].

The dilation and constriction of the pupil are dominated by the sympathetic and parasympathetic nerves from the autonomic nervous system [34]. Therefore, the pupil diameter marker PDM has been recommended as a credible indicator for psychophysiological state estimation in HMI studies [29], [34], [35]. In this research, the generated pupil size is the mean value from 30-second image frameworks. It is generated from the mean value of both eyes, based on a pixel calculation, relative distance measurement and head movement scale factor from captured images. Previous studies have found that psychophysiological change can impact human thermoregulation and lead to perceptible changes in skin temperature [36], [37]. This research focuses on the temperature information extracted from the forehead, periorbital and nasal regions of the participants. The psychophysiological biomarkers developed based on these data are the mean forehead temperature $\bar{T_f}$, the maximum facial temperature T_{maxf} and the mean nasal temperature $\bar{T_n}$. The effectiveness and efficiency of these facial temperature biomarkers in HMI were validated in [30]. The sampling frequency of the thermal camera is 10 Hz, and the values of the biomarkers are the averages in a 15-second period window.

III. Adaptive General Type-2 Fuzzy Modelling

The psychophysiological state of a subject in HMI consists of both inner consciousness and outer behaviour. This requires the model to be adaptive to continuous observations and self-adjust its structures and parameters as the participant's psychophysiological states evolve with time. Therefore, it would be difficult to find the associated conventional mathematical model representations. Existing models and frameworks for predicting the psychophysiological state include the adaptive neuro-fuzzy inference system (ANFIS), Mamdani-type fuzzy model, proportional integral Mamdani fuzzy model, type-2 fuzzy model and support vector machines (SVMs) [5]–[7], [10], [12], [14], [16], [17]. ANFIS models often suffer from overfitting problems because of a lack of adaptation. SVM models need to specify kernel functions for individuals to optimise feature extraction. Mamdani-type fuzzy models are transparent and more efficient in describing the subjective part of the state. Compared to the other models, the type-2 fuzzy models have achieved the best prediction results so far because they can handle uncertainty with a lower data requirement and are usually less prone to overfitting.

Fuzzy logic models are capable of handling a large amount of uncertainty and demonstrate great flexibility in modelling nonlinear systems [5]–[7], [9]–[18], [38], [39]. A type-2 fuzzy model is capable of dealing with the heuristic or linguistic uncertainty within the system. Additionally, it can also be tolerant of random uncertainties that limit current predictive approaches. The systems based on type-2 fuzzy sets are effective in cases where there are uncertainties in both the rule and the measurement [38], [40], [41].

The human psychological responses to the same stimulus are individual dependent. Hence, an adaptive general type-2 fuzzy framework is selected and devised to exploit the advantage of type-2 fuzzy logic to handle the intra- and inter-uncertainty while achieving fast adaptive learning with Bayes' theorem. The model first predicts the trend of the subject's future performance based on the latest records. The type-2 fuzzy framework takes psychophysiological data as the input and uses the centre-of-sets (COS) type-reduction method to generate the initial prediction of each fired fuzzy rule that can be easily interpreted by humans. The final prediction of modelling combines all the predictions with the performance trend. When the final prediction varies from the actual observed value, the selected fuzzy rule from the rule base is recursively updated with the observation in a Bayesian function [42].

One example fuzzy rule of the adaptive general type-2 fuzzy model (GT2FM) before the experiment is illustrated in Figure 1, where the shaded area represents the footprint of the first degree uncertainty, and its corresponding linguistic form reads as follows:

Rule 1: ***IF*** *$\bar{T_n}$ is large, $\bar{T_f}$ is medium, T_{maxf} is small, HRV_1 is small, HRV_2 is large, TLI_1 is large, TLI_2 is small, and PDM is large,* ***THEN*** *the task accuracy is small.*

The first degree of uncertainty of the fuzzy rule remains fixed during the inference, whereas the second degree of uncertainty keeps varying with the current state. Table I summarises two sample fuzzy rules of the adaptive general type-2 fuzzy model, which describe the relationships between the inputs and output under the condition of the same difficulty level (data based on the previous research in [30]). The linguistic labels

TABLE I
RULE BASE OF GT2FM FOR THE FIRST STATE

	Inputs									Output
	T_n	T_f	T_{maxf}	HRV_1	HRV_2	TLI_1	TLI_2	PDM	$DifficultyLevel$	$TaskAccuracy$
Rule 1	Large	Medium	Small	Small	Large	Large	Small	Large	0.25	Small
Rule 2	Medium	Large	Medium	Large	Small	Medium	Medium	Small	0.25	Large

TABLE II
LINGUISTIC LABELS OF THE INPUTS AND OUTPUT FOR THE FIRST STATE

Linguistic Labels	T_n	T_f	T_{maxf}	HRV_1	HRV_2	TLI_1	TLI_2	PDM	$TaskAccuracy$
Small	<33.5	<33.9	<36.0	<0.37	<0.18	<0.18	<0.28	<0.14	<0.72
Medium	33.5-34.1	33.9-34.1	36.0-36.1	0.37-0.53	0.18-0.23	0.18-0.29	0.28-0.30	0.14-0.16	0.72-0.97
Large	>34.1	>34.1	>36.1	>0.53	>0.23	>0.30	>0.30	>0.16	>0.97

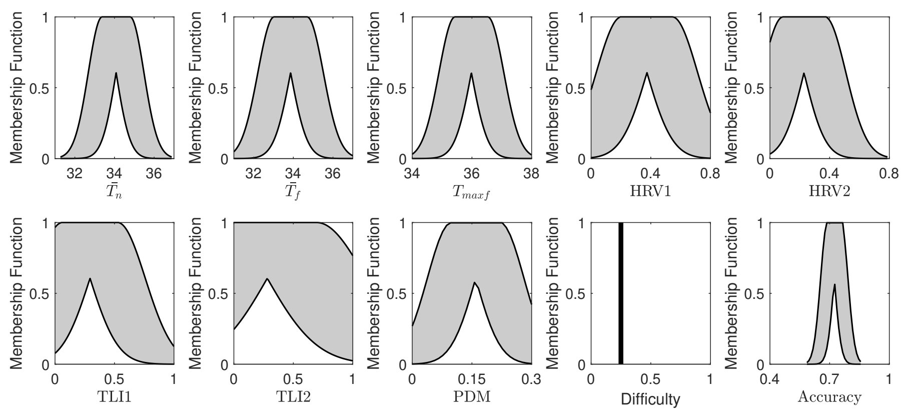

Fig. 1. Example initial rule of GT2FM for the first state

applied in the fuzzy rules are illustrated in Table II.

The following steps explain the inference mechanism leading to an output:

1) Calculate the latest transition matrix P for each state; in a period of time, different task performance ranges indicate different K states of the subject (the states describe the performance in descending order). The entries in the first row of the transition matrix P represent the probability for the adjacent two states 0 & 2 and the same state 1 following the first state 1 (task performance measurement is continuous), and similarly for the remaining rows:

$$P = \begin{bmatrix} P_{(1,0)} & P_{(1,1)} & P_{(1,2)} \\ P_{(2,1)} & P_{(2,2)} & P_{(2,3)} \\ & \vdots & \\ P_{(K,K-1)} & P_{(K,K)} & P_{(K,K+1)} \end{bmatrix}, \quad (2)$$

$$P_{(S_n=i,S_{n+1}=j)} = P_{(S_{n+1}=j|S_n=i)} \cdot P_{(S_n=i)}, \quad (3)$$

where $P_{(i,j)}$ is estimated via Equation 3 in a certain amount of time, except $P_{(1,0)} = P_{(K,K+1)} = 0$. $P_{(S_n=i)}$ represents the total probability of initial state i, and $P_{(S_{n+1}=j|S_n=i)}$ represents the probability of state j given the initial state i.

2) Perform the state estimation E for the current time t with the transition matrix P. The following gives the expectation of each state to be presented at the time t:

$$E_t = \begin{bmatrix} E_{(t,1)} & \dots & E_{(t,i)} & \dots & E_{(t,K)} \end{bmatrix}, \quad (4)$$

$$E_t = E_{t-1} \cdot P_{t-1}, \quad (5)$$

where $E_{(t,i)}$ denotes the expectation of state i at the time t.

3) Compute the upper and lower membership functions $\overline{F}$ & $\underline{F}$ for firing the fuzzy rules. The rule base R consists of $4K$ fuzzy rules describing each state with M different difficulty levels:

$$R = \begin{bmatrix} R_{(1,1)} & \dots & R_{(1,K)} \\ \vdots & \ddots & \\ R_{(M,1)} & & R_{(M,K)} \end{bmatrix}, \quad (6)$$

where $R_{(i,j)}$ represents the fuzzy rule describing the state j at the difficulty level i. The input values of each rule are range values with means μ_x and standard deviations σ_x, representing the measurement uncertainty and individual difference. The firing of the fuzzy rules involves the K fuzzy rules covering every state of the participants for the difficulty levels that they currently experience. The inference between the input values and one firing fuzzy rule depends on Gaussian functions, and for simplification, the functions have the same standard deviation value from that rule. The following summarises the inference processes to find the upper and lower membership functions $\overline{f}$ & $\underline{f}$ for one single input x and one firing fuzzy rule:

a) if $x < \mu_x - \sigma_x$, then find m and n that satisfy:

$$\begin{aligned} f(m|x,\sigma_x^2) &= f(m|\mu_x + \sigma_x, \sigma_x^2), \\ f(n|x,\sigma_x^2) &= f(n|\mu_x - \sigma_x, \sigma_x^2), \end{aligned} \tag{7}$$

where

$$f(\bar{x}|\mu,\sigma^2) = \frac{1}{\sigma\sqrt{2\pi}} e^{-(\bar{x}-\mu)^2/2\sigma^2}, \tag{8}$$

which gives

$$\begin{aligned} \underline{f} &= \frac{f(m|x,\sigma_x^2)}{f(x|x,\sigma_x^2)}, \\ \overline{f} &= \frac{f(n|x,\sigma_x^2)}{f(x|x,\sigma_x^2)}; \end{aligned} \tag{9}$$

b) if $\mu_x - \sigma_x \leq x \leq \mu_x + \sigma_x$, then find l that satisfies:

$$f(l|x,\sigma_x^2) = f(l|\mu_x, \sigma_x^2), \tag{10}$$

which gives

$$\begin{aligned} \underline{f} &= \frac{f(l|x,\sigma_x^2)}{f(x|x,\sigma_x^2)}, \\ \overline{f} &= 1; \end{aligned} \tag{11}$$

c) if $\mu_x + \sigma_x < a$, then find m and n that satisfy:

$$\begin{aligned} f(m|x,\sigma_x^2) &= f(m|\mu_x - \sigma_x, \sigma_x^2), \\ f(n|x,\sigma_x^2) &= f(n|\mu_x + \sigma_x, \sigma_x^2), \end{aligned} \tag{12}$$

which gives the result presented in equation 9.

In this way, the final membership functions for one firing fuzzy rule $\overline{F}$ & $\underline{F}$ are

$$\begin{aligned} \underline{F} &= \left\{ \max(\underline{f}_i) | \forall i \in L \right\}, \\ \overline{F} &= \left\{ \max(\overline{f}_i) | \forall i \in L \right\}, \end{aligned} \tag{13}$$

where L represents the number of inputs.

4) Find the initial prediction of each firing fuzzy rule with the transition matrix P and the membership functions F. Similar to the input values, each fuzzy rule has a range for the output values $\forall y \in [\underline{y}, \overline{y}]$. The following summarises the type-reduction processes to find the prediction value y_k for one firing fuzzy rule k with the transition matrix P and membership function F (sort $\underline{y}$ & $\overline{y}$ in ascending order):

a) if $P_{(k,k-1)} < P_{(k,k+1)}$ or for the fuzzy rule representing the last state $P_{(k,k-1)} < P_{(k,k)}$, then

$$y_k = \frac{\sum_{n=1}^{k} \overline{F}^n \cdot \underline{y}^n + \sum_{n=k+1}^{K} \underline{F}^n \cdot \underline{y}^n}{\sum_{n=1}^{k} \overline{F}^n + \sum_{n=k+1}^{K} \underline{F}^n}, \tag{14}$$

b) if $P_{(k,k+1)} < P_{(k,k-1)}$ or for the fuzzy rule representing the first state $P_{(k,k+1)} < P_{(k,k)}$, then

$$y_k = \frac{\sum_{n=1}^{k-1} \underline{F}^n \cdot \overline{y}^n + \sum_{n=k}^{K} \overline{F}^n \cdot \overline{y}^n}{\sum_{n=1}^{k-1} \underline{F}^n + \sum_{n=k}^{K} \overline{F}^n}, \tag{15}$$

c) if $P_{(k,k-1)} = P_{(k,k+1)}$ or for the fuzzy rule representing any middle state $P_{(k,k)} > \max(P_{(k,k-1)}, P_{(k,k+1)})$ or for both fuzzy rules representing two end states $P_{(k,k)} = P_{(k,k-1)} + P_{(k,k+1)}$, then

$$\begin{aligned} y_{(k,l)} &= \frac{\sum_{n=1}^{k} \overline{F}^n \cdot \underline{y}^n + \sum_{n=k+1}^{K} \underline{F}^n \cdot \overline{y}^n}{\sum_{n=1}^{k} \overline{F}^n + \sum_{n=k+1}^{K} \underline{F}^n}, \\ y_{(k,h)} &= \frac{\sum_{n=1}^{k} \underline{F}^n \cdot \overline{y}^n + \sum_{n=k+1}^{K} \overline{F}^n \cdot \underline{y}^n}{\sum_{n=1}^{k} \underline{F}^n + \sum_{n=k+1}^{K} \overline{F}^n}, \\ y_k &= \frac{y_{(k,l)} + y_{(k,h)}}{2}. \end{aligned} \tag{16}$$

The main idea of the type-reduction algorithm is to keep the prediction consistently corresponding to the tendency measured from the state tracking. Taking Equation (15) as an example, y_k is a maximised prediction. Since the probability of switching to a better state dominates, the likelihood for $\overline{y}^n$ from a back state decreases, and for $\overline{y}^n$ from a front state increases. For $n < k$, the y_k calculation uses the lower membership weights; for $n \geq k$, the y_k calculation uses the upper membership weights. This algorithm ensures that the prediction is maximised by the transition matrix.

5) Generate the final prediction $\hat{y}_t$ from the state estimations E_t and the initial predictions $y_{(t,k)}$. The following gives the final prediction of the model at time t:

$$Y_t = \begin{bmatrix} y_{(t,1)} & y_{(t,2)} & \dots & y_{(t,K)} \end{bmatrix}, \tag{17}$$

$$\hat{y}_t = Y_t \cdot E_t^{\mathsf{T}}, \tag{18}$$

where Y_t denotes the set of all individual predictions from every firing fuzzy rule at time t.

The adaptive general type-2 fuzzy modelling algorithm uses two fuzzy membership sets for the prediction computation. The primary membership represents the individual difference and measurement uncertainty. The type-reduction in the primary membership weights is based on participant state tracking, which forms the secondary membership sets of the model. This membership is computed by comparing the input vector to the selected fuzzy rules, and the prediction is generated based on the latest state information. The modelling algorithm utilises a simplified inference to combine the statistical estimation and the fuzzy logic mechanism. Thus, it considers the data uncertainty and aligns this uncertainty with the forecast without a computationally expensive type-reduction algorithm that limits the use of general type-2 fuzzy logic sets [40]. In addition, intra-uncertainty is integrated with the framework by a simplified learning algorithm. Intra-uncertainty develops with time and gradually reduces the reliability of the model. Therefore, an adaptive learning algorithm based on the Bayes' theorem [42] is implemented for updating the rule base.

The adaptive learning algorithm follows the following steps:

1) Calculate the prediction error and check it with the maximum error tolerance ET_{max}. The adaptive learning algorithm is only applied if the error between the prediction $\hat{y}_{t-1}$ and the observation o_{t-1} at time t-1 exceeds the limitation:

$$\|\hat{y}_{t-1} - o_{t-1}\| > ET_{max} \tag{19}$$

2) When the learning algorithm is needed, update the selected fuzzy rule with the observation o_{t-1} using the Bayes' theorem [42]. The selected fuzzy rule has the same subject state under the same difficulty level as the observation o_{t-1}, with the means μ_{t-1} and the standard deviations σ_{t-1} for the inputs and output. The observation o_{t-1} is described with Gaussian functions with the means $\mu_{o,t-1}$ and the standard deviations $\sigma_{o,t-1}$. The posterior mean and the posterior standard deviation of the conjugate prior for the normal distribution are calculated as follows:

$$\begin{aligned} E(\mu_t|\mu_{o,t-1}) &= \frac{\sigma_{t-1}^2 \cdot \mu_{t-1} + \sigma_{o,t-1}^2 \cdot \mu_{o,t-1}}{\sigma_{t-1}^2 + \sigma_{o,t-1}^2}, \\ Var(\sigma_t|\sigma_{o,t-1}) &= \frac{\sigma_{t-1}^2 \cdot \sigma_{o,t-1}^2}{\sigma_{t-1}^2 + \sigma_{o,t-1}^2}, \end{aligned} \tag{20}$$

where $\sigma_{o,t-1}$ is equal to the initial value of standard deviations of the fuzzy rule, considering the individual difference and measurement uncertainty is time independent.

3) Calculate the distance between the new fuzzy rule and the observation and check it with the maximum distance tolerance DT_{max}:
   a) if $\|\mu_t - \mu_{o,t-1}\| > DT_{max}$, replace μ_{t-1} & σ_{t-1} with μ_t & σ_t and repeat the Bayesian update;
   b) else if $\|\mu_t - \mu_{o,t-1}\| \leq DT_{max}$, stop the learning algorithm and replace the old fuzzy rule with the new rule.

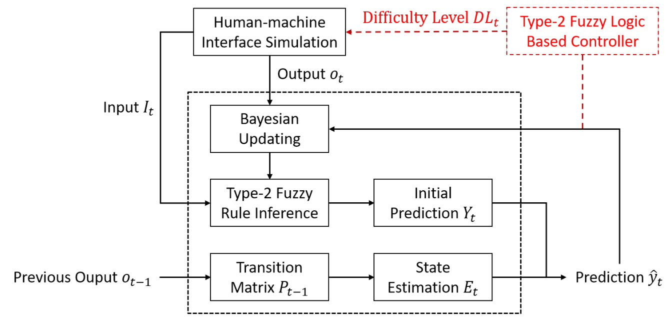

Fig. 2. Diagram of the GT2FM for the HMI simulation experiment (controller and other sections in - - are the subject of the following study)

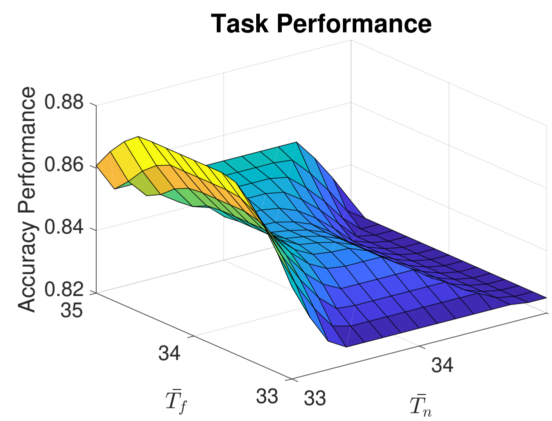

Fig. 3. Membership for the performance function $f_A(\bar{T}_n, \bar{T}_f)$

IV. Experimental Results

This section focuses on the prediction results of the adaptive general type-2 fuzzy framework mentioned in Sections III. The model is implemented in HMI mental arithmetic experiments for online real-time predictions. This section also includes the prediction results of a generalised off-line ANFIS model and the real-time A-GT2-FCM model based on the same experimental data for comparison. The evaluations and summaries of the experimental results in the following section should demonstrate the performance of the system.

A. Model Configuration

The adaptive general type-2 fuzzy model (GT2FM) was built using the computational frameworks of MATLAB®. The HMI mental arithmetic experiment includes four different difficulty levels $M = 4$. In this research, the input vector for the system is $I(t) = [HRV_1(t),\ HRV_2(t),\ TLI_1(t),\ TLI_2(t),\ PDM(t),\ \bar{T}_n(t),\ \bar{T}_f(t),\ T_{maxf}(t),\ DL(t)]$. The corresponding output of the HMI simulation system is the actual accuracy $o(t)$, which is also recorded as the observation for the prediction at time $t+1$. The prediction output of the model is the predicted accuracy $\hat{y}(t)$. Figure 2 shows the diagram of the GT2FM that was designed for the HMI simulation.

The GT2FM model starts to generate the prediction 30 seconds after the experiment begins. The computational framework consists of a total of eight (8) fuzzy rules, which leads to two (2) fuzzy rules per difficulty level and divides the operator task performance into two states. The root mean square standardised error e_{rmsse} is introduced to evaluate the complexity of the model and to compare it with the real HMI simulation results as follows:

$$e_{rmsse} = \sqrt{\frac{\sum_{i=1}^{n}[(\hat{y}_i - o_i)/\hat{\sigma}_o]^2}{n}}, \tag{21}$$

where $\hat{\sigma}_o$ is the standard error of the observations, and n is the length of the data. The mean error for ten participants is $e_{RMSSE} = 0.1376 < 1$, which indicates that the variability of the model should satisfy the HMI prediction with no need for dividing any extra state to introduce a more fuzzy rule.

The generalised off-line ANFIS model is constructed and trained with the MATLAB®built-in functions *genfis* and *anfis*. The model implements fuzzy c-means (FCM) for each participant, dividing 5 clusters for each input. The ANFIS model is trained with all the experimental data from the first session and then validated with the individual data from the second session for each participant. The real-time A-GT2-FCM model is the same model applied in previous research [16]. The error tolerance ET_{max} of the A-GT2-FCM model is set to 0.01, the same as the GT2FM model.

B. Modelling Results

As described in Section II, one experiment consists of two HMI mental arithmetic sessions for real-time modelling. The participant undergoes the first session with incremental difficulty levels and then the following second session with randomised difficulty levels, with a 5-minute interval.

The model framework starts with an initial rule base from the generalised results in the previous experiment [30], with the first state estimation matrix $E_1 = [1\ 0]$ and the first transition matrix $P = [1\ 0;\ 0\ 1]$. Figure 3 shows the membership function between the task performance and two facial temperature readings $\bar{T_n}$ and $\bar{T_f}$, which is based on the two initial fuzzy rules for describing the first state. The shadow plot of the example fuzzy rule from the GT2FM after the experiment is presented in Figure 4. The adaptive learning algorithm thereupon calculates the new state estimation and elicits the new individual dependent fuzzy rules according to the psychophysiological recordings and the observations.

The Pearson correlations c and the root mean squared error e_{rmse} are introduced to assess the prediction of the adaptive general type-2 fuzzy model. Table III shows the correlations and the errors between the observations and the predictions for each participant in each session. The calculations of these indices for n samples are via the following equations:

$$\begin{aligned} c_{\hat{y},o} &= \frac{1}{n-1}\sum_{i=1}^{n}(\frac{\hat{y}_i - \mu_{\hat{y}}}{\sigma_{\hat{y}}})(\frac{o_i - \mu_o}{\sigma_o}), \\ e_{rmse} &= 100 \cdot \sqrt{\frac{\sum_{i=1}^{n}(\hat{y}_i - o_i)^2}{n}}, \end{aligned} \tag{22}$$

where $\mu_{\hat{y}}$ and $\sigma_{\hat{y}}$ are the mean and standard deviation of the prediction $\hat{y}$, respectively, and μ_o and σ_o are the mean and standard deviation of observation o. The sampling rate for the model is 1 Hz, so the total number of samples for one session is $n = 690$.

Tables III, IV and V summarise the prediction results for all the participants from the real-time online modelling of GT2FM and A-GT2-FCM and the off-line generalised ANFIS. In Table III, it can be seen that the mean correlations and the mean errors of the GT2FM remain consistent. Compared to the A-GT2-FCM (Table IV) and the ANFIS models (Table V), the prediction results of GT2FM have the highest correlations and the lowest error rates across all participants. Overall, the GT2FM model performs well and consistently throughout the entire experiment. Based on the prediction outcome, the GT2FM model presents an excellent predictive ability due to the forecast prediction of the participant's state. The learning algorithm is capable of fast individual feature extraction without any prior knowledge or specific training. To further evaluate the ability of the model, Figures 5 and 6 show the detailed time sequences of the prediction and the psychophysiological biomarkers for participant no. 08 in both sessions.

From the task performance plot of Figure 5, compared to the A-GT2-FCM and ANFIS model, the predictions of the GT2FM match the actual performance of the participant the most. It can be seen how fast the adaptive general type-2 fuzzy model adjusts itself at the beginning of the experiment. This plot also shows the GT2FM model capability of handling high-frequency state change from the last phase. The psychophysiological inputs for all the models are presented in Figure 5. It is worth noting that all the psychophysiological biomarkers suffer from a certain degree of delay in representing the participant's inner state. However, the GT2FM model can still maintain the delay within 1 to 2 seconds throughout all participants in this research despite the intra-parameter variations. Merging the existing fuzzy rules and the observations keeps the rule base simple and up-to-date. It ensures the efficiency and effectiveness of the prediction inference process.

The psychophysiological biomarker readings (HRV_1, HRV_2, TLI_1, TLI_2, PDM, $\bar{T_n}$, $\bar{T_f}$, T_{maxf} and DL) in Figures 5 and 6 have been normalised for the purpose of

TABLE III
CORRELATIONS AND ROOT MEAN SQUARED ERRORS (RMSE) FOR REAL ACCURACY VERSUS PREDICTED ACCURACY OF GT2FM

Participant	Correlation (%)		Root Mean Squared Error (%)	
	Session 1	Session 2	Session 1	Session 2
01	98.75	99.55	3.628	2.430
02	98.33	98.85	1.725	1.476
03	99.52	99.42	2.265	2.237
04	99.60	99.40	2.205	1.982
05	98.19	98.69	4.109	3.635
06	99.50	99.37	2.504	2.773
07	98.91	99.07	2.081	2.208
08	98.62	99.12	2.276	2.392
08	98.29	98.96	2.365	1.972
10	98.67	99.22	2.192	1.706
Mean	98.84	99.17	2.535	2.281

TABLE IV
CORRELATIONS AND ROOT MEAN SQUARED ERRORS (RMSE) FOR REAL ACCURACY VERSUS PREDICTED ACCURACY OF A-GT2-FCM

Participant	Correlation (%)		Root Mean Squared Error (%)	
	Session 1	Session 2	Session 1	Session 2
01	97.06	98.15	5.536	4.977
02	95.43	97.34	2.931	2.375
03	98.21	97.70	4.957	4.541
04	98.67	97.53	4.201	4.159
05	95.66	96.76	6.505	5.995
06	98.80	97.95	3.965	5.086
07	97.04	98.50	3.583	2.877
08	96.45	97.19	3.710	4.398
08	96.69	97.25	3.397	3.387
10	97.39	98.19	3.178	2.758
Mean	97.14	97.66	4.198	4.058

TABLE V
CORRELATIONS AND ROOT MEAN SQUARED ERRORS (RMSE) FOR REAL ACCURACY VERSUS PREDICTED ACCURACY OF ANFIS

Participant	Correlation (%)		Root Mean Squared Error (%)	
	Session 1	Session 2	Session 1	Session 2
01	80.63	72.27	13.740	18.590
02	70.02	57.24	6.828	52.290
03	84.88	59.18	12.280	22.800
04	96.76	73.32	6.223	47.430
05	80.74	72.89	12.800	20.460
06	90.99	-32.54	10.800	82.180
07	75.95	91.37	9.326	8.505
08	75.97	22.89	8.987	23.640
08	84.38	79.68	7.793	15.350
10	93.12	56.76	4.961	37.030
Mean	83.34	61.81	9.374	32.828

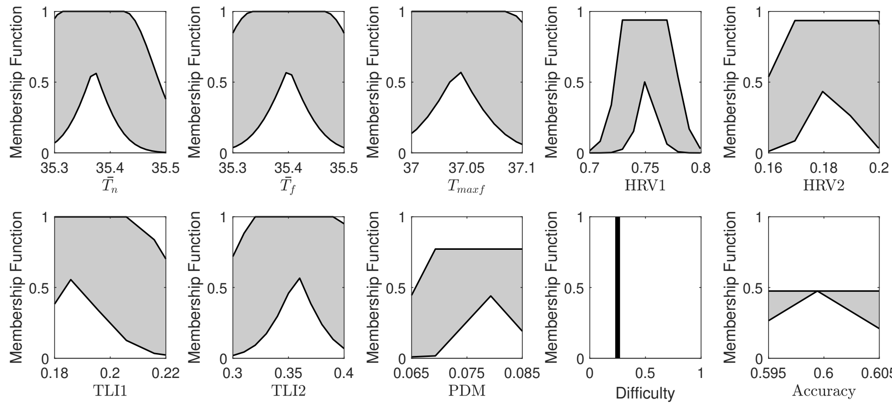

Fig. 4. Example final rule of GT2FM for the first state

illustration only. The adaptive general type-2 fuzzy model does not require any type of normalisation to operate.

C. Adaptive Learning of the Adaptive General Type-2 Fuzzy Model

Table III, Figures 5, 6 and 7 illustrate the adaptive learning of the adaptive general type-2 fuzzy model via comparisons between the predictions and the observation. As already stated in Section III, the GT2FM combines the inter- and intra-uncertainty within the type-2 fuzzy sets. The state tracking algorithm finalises the prediction according to the trend estimation and the probability. The learning algorithm keeps the fuzzy rule configuration consistent with the current situation. In this research, the adaptive learning of the adaptive general type-2 fuzzy model can be interpreted as follows.

The model can self-organise in real time. In the task performance plots of Figures 5, 6 and 7, it can be observed that the model quickly adjusts at the beginning of the experiment and when the participant's performance becomes unstable. The psychophysiological indices of the participants vary with multiple factors in addition to the task load. Thus, the psychophysiological recordings demonstrate clearly different patterns even for the same person with the same difficulty level (e.g., the psychophysiological recordings plots of Figures 5 and 6). However, similar performances from all participants suggest that the learning and self-organising abilities of the model are sufficient for this intra-uncertainty.

The model is generalised for every participant. The model does not require individual-based calibration or off-line training for operation. The initial rule base, the first state estimation matrix and the first transition matrix are universal for all the participants. It is worth noting that the initial rule base is based on sample mathematical estimations from previous inputs and output data. The initial statistical means and deviations only influence the speed of the convergence rather than itself. Despite having uncertainty from participant to participant and among participants, the model succeeds in extracting these uncertainties and transferring them into recognisable patterns. For example, comparing the psychophysiological biomarker recordings in Figures 6 and 7, there are significant differences between these biomarker values even when participants 03 and 08 are under the same experimental conditions. It can also be observed that participant 08 shows higher values than participant 03 in all the facial temperature indicators $\bar{T}_n$, $\bar{T}_f$ and T_{maxf}. $HRV1$ provides another evident inter-subject variation. Compared with the indicators from participant 03, these $HRV1$ values of participant 08 are doubled. This can explain the performance differences within the participants based on the work-memory theory. Inter-differences in the predicted accuracy at the beginning of the prediction in the task performance plot are also obvious. This suggests that the initial rule base describes participant 03 more precisely than for participant 08.

The model can manage temporal information loss and noise. In the real-time HMI simulation experiment, information losses occasionally occur because of sudden disconnections between the electrodes and the subject. Additionally, noise is introduced with task-irrelevant events such as unconscious movement. The red circles in Figures 6 and 7 represent the cases of information loss. The noise within the recordings can be conspicuous and might be persistent throughout the whole session. One extreme example can be found in the psychophysiological recording plots for PDM in Figure 6; the value drops to nearly 0 during the first phase, which is clearly impossible for pupils and can only be a misinterpretation for something else. However, the model manages to maintain high accuracy during these periods from the task performance plots of Figures 6. The combination of different biomarkers provides the model with the ability to quickly switch the lead biomarkers, it depends on and maintains the consistency of the model prediction. In some extreme cases where all the facial temperature biomarkers $\bar{T}_n$, $\bar{T}_f$ and T_{maxf} are removed from the model input vector, the time lag between the model prediction and the observation still remains within three seconds.

V. Conclusion

This study focused on the prediction of the human operator psychophysiological state in the HMI system. Mental arithmetic was selected as the simulation of HMI systems for 10

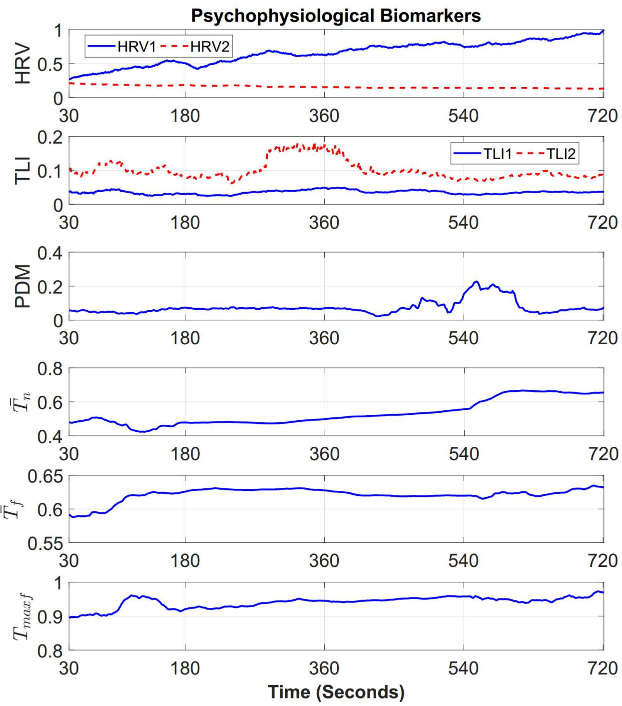

(a) Psychophysiological biomarker recordings (HRV1, HRV2, TLI1, TLI2, PDM, $\bar{T_n}$, $\bar{T_f}$, T_{maxf})

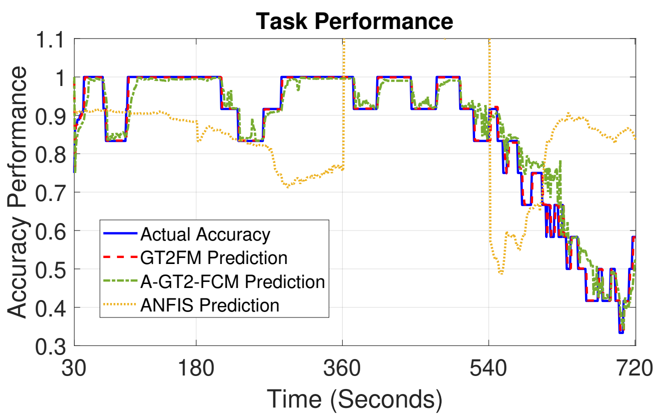

(b) Accuracy performance from participant 08 and from the adaptive general type-2 fuzzy model prediction

Fig. 5. Real-time experiment results and model predictions for participant 08 in session 2

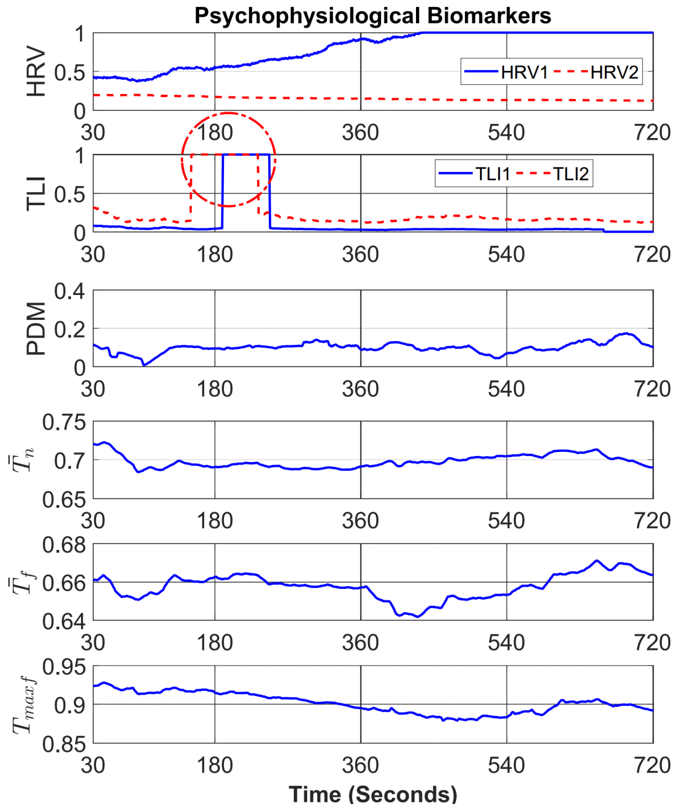

(a) Psychophysiological biomarker recordings (HRV1, HRV2, TLI1, TLI2, PDM, $\bar{T_n}$, $\bar{T_f}$, T_{maxf})

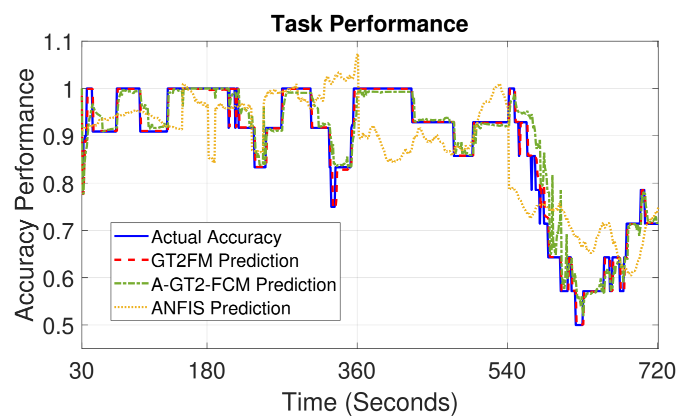

(b) Accuracy performance from participant 08 and from the adaptive general type-2 fuzzy model prediction

Fig. 6. Real-time experimental results and model predictions for participant 08 in session 1

participants. In addition to the previous psychophysiological biomarkers TLI, HRV and pupil diameter, new facial temperature indicators were introduced and integrated with others for assessing the operators' psychophysiological state.

A new modelling approach named adaptive general type-2 fuzzy modelling was proposed to predict human psychophysiological state based on real-time experiments. Such a new modelling approach integrated system uncertainty with type-2 fuzzy sets and state tracking with defuzzification to estimate the human psychophysiological state. The model prediction results were compared to participant-specific ANFIS and A-GT2-FCM, and it was found that the proposed model outperformed the other models presented in the related literature. The design of an adaptive learning algorithm based on Bayes' theorem proved its ability to extract patterns from observations in real time. With the estimation and classification of psychophysiological state, high accuracy and reasonable correlation were achieved even for breakdown periods.

In summary, the results of this study provided an evaluation for applying adaptive general type-2 fuzzy modelling to systems similar to HMI. Furthermore, it created the foundation for more advanced control mechanisms for HMI systems and can be applied for the exploration of the origins of human operator compromised performance in the future.

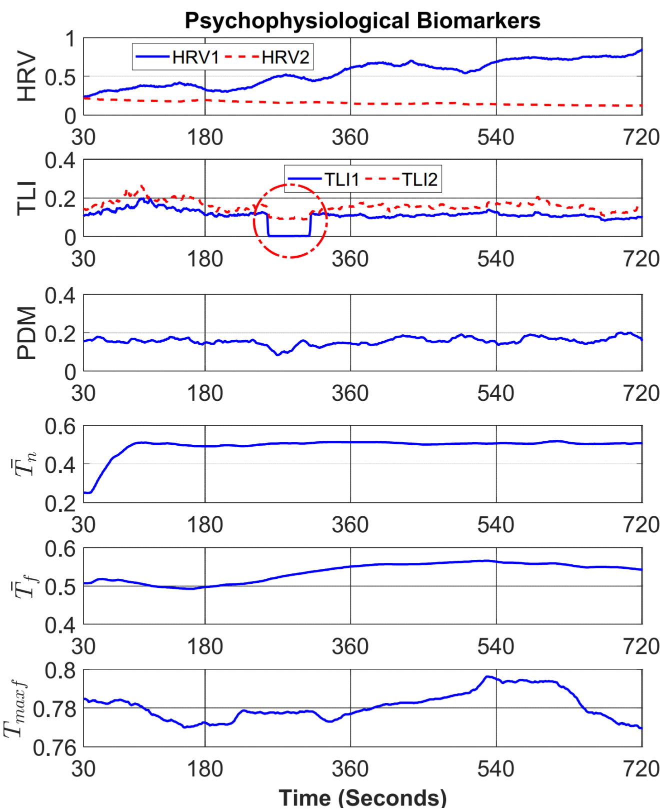

(a) Psychophysiological biomarker recordings (HRV1, HRV2, TLI1, TLI2, PDM, $\bar{T}_n$, $\bar{T}_f$, T_{maxf})

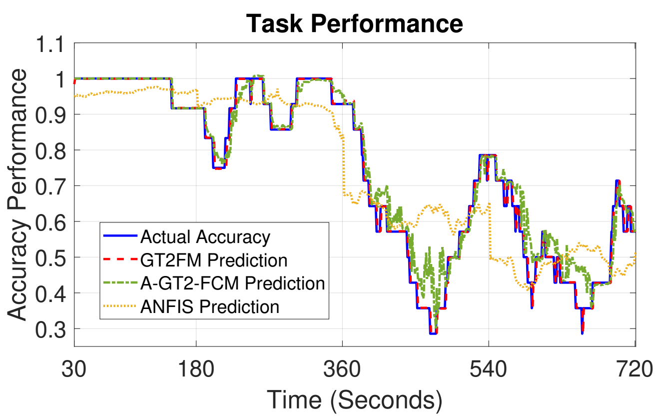

(b) Accuracy performance from participant 03 and from the adaptive general type-2 fuzzy model prediction

Fig. 7. Real-time experiment results and model predictions for participant 03 in session 1

REFERENCES

[1] S. Walter, C. Wendt, J. Böhnke, S. Crawcour, J.-W. Tan, A. Chan, K. Limbrecht, S. Gruss, and H. C. Traue, "Similarities and differences of emotions in human–machine and human–human interactions: what kind of emotions are relevant for future companion systems?" *Ergonomics*, vol. 57, no. 3, pp. 374–386, 2014.

[2] S. Feit, N. Scheufler, D. Choi, M. Kosterich, R. Miller, C. Grebe, and J. Lin, "Predictive human-machine interface using eye gaze technology, blind spot indicators and driver experience," May 16 2017, uS Patent 9,650,041.

[3] Y. Li, K. He, X. Sun, and H. Liu, "Human-machine interface based on multi-channel single-element ultrasound transducers: A preliminary study," in *2016 IEEE 18th International Conference on e-Health Networking, Applications and Services (Healthcom)*. IEEE, 2016, pp. 1–6.

[4] I. B. Mauss and M. D. Robinson, "Measures of emotion: A review," *Cognition and emotion*, vol. 23, no. 2, pp. 209–237, 2009.

[5] A. Gevins and M. E. Smith, "Neurophysiological measures of cognitive workload during human-computer interaction," *Theoretical Issues in Ergonomics Science*, vol. 4, no. 1-2, pp. 113–131, 2003.

[6] K. Hong and S. Hong, "Real-time stress assessment using thermal imaging," *The Visual Computer*, vol. 32, no. 11, pp. 1369–1377, 2016.

[7] M. Mahfouf, J. Zhang, D. A. Linkens, A. Nassef, P. Nickel, G. R. J. Hockey, and A. C. Roberts, "Adaptive fuzzy approaches to modelling operator functional states in a human-machine process control system," in *Fuzzy Systems Conference, 2007. FUZZ-IEEE 2007. IEEE International*. IEEE, 2007, pp. 1–6.

[8] ——, "Adaptive fuzzy approaches to modelling operator functional states in a human-machine process control system," in *Fuzzy Systems Conference, 2007. FUZZ-IEEE 2007. IEEE International*. IEEE, 2007, pp. 1–6.

[9] A. Nassef, C.-H. Ting, M. Mahfouf, D. A. Linkens, P. Nickel, G. R. J. Hockey, and A. C. Roberts, "A new framework for real-time adaptive fuzzy monitoring and control for humans under psychophysiological stress." in *BIOSIGNALS (2)*, 2008, pp. 320–325.

[10] A. Nassef, M. Mahfouf, C.-H. Ting, E. El-Samahy, D. A. Linkens, and M. A. Denaï, "Hybrid physiological modeling of subjects undergoing cyclic physical loading." in *Biosignals*, 2010, pp. 252–257.

[11] A. Nassef, M. Mahfouf, D. Linkens, E. Elsamahy, A. Roberts, P. Nickel, G. Hockey, and G. Panoutsos, "The assessment of heart rate variability (hrv) and task load index (tli) as physiological markers for physical stress," in *World Congress on Medical Physics and Biomedical Engineering, September 7-12, 2009, Munich, Germany*. Springer, 2009, pp. 146–149.

[12] E. El-Samahy, M. Mahfouf, L. Torres-Salomao, and J. Anzurez-Marin, "A new computer control system for mental stress management using fuzzy logic," in *Evolving and Adaptive Intelligent Systems (EAIS), 2015 IEEE International Conference on*. IEEE, 2015, pp. 1–7.

[13] C.-H. Ting, M. Mahfouf, D. A. Linkens, A. Nassef, P. Nickel, A. C. Roberts, M. H. Roberts, and G. R. J. Hockey, "Real-time adaptive automation for performance enhancement of operators in a human-machine system," in *Control and Automation, 2008 16th Mediterranean Conference on*. IEEE, 2008, pp. 552–557.

[14] C.-H. Ting, M. Mahfouf, A. Nassef, D. A. Linkens, G. Panoutsos, P. Nickel, A. C. Roberts, and G. R. J. Hockey, "Real-time adaptive automation system based on identification of operator functional state in simulated process control operations," *IEEE Transactions on Systems, Man, and Cybernetics-Part A: Systems and Humans*, vol. 40, no. 2, pp. 251–262, 2010.

[15] L. A. Torres-Salomao, M. Mahfouf, and O. Obajemu, "Interval type-2 fuzzy logic adaptive modelling for human operators undergoing mental stress," *IFAC Proceedings Volumes*, vol. 47, no. 3, pp. 9880–9885, 2014.

[16] L. A. Torres-Salomao, M. Mahfouf, E. El-Samahy, and C.-H. Ting, "Psychophysiologically based real-time adaptive general type 2 fuzzy modeling and self-organizing control of operator's performance undertaking a cognitive task." *IEEE Trans. Fuzzy Systems*, vol. 25, no. 1, pp. 43–57, 2017.

[17] J. Zhai and A. Barreto, "Stress detection in computer users based on digital signal processing of noninvasive physiological variables," in *Engineering in Medicine and Biology Society, 2006. EMBS'06. 28th Annual International Conference of the IEEE*. IEEE, 2006, pp. 1355–1358.

[18] J. Zhai, A. B. Barreto, C. Chin, and C. Li, "Realization of stress detection using psychophysiological signals for improvement of human-computer interactions," in *SoutheastCon, 2005. Proceedings. IEEE*. IEEE, 2005, pp. 415–420.

[19] J. J. Bird, L. J. Manso, E. P. Ribeiro, A. Ekart, and D. R. Faria, "A study on mental state classification using eeg-based brain-machine interface," in *2018 International Conference on Intelligent Systems (IS)*. IEEE, 2018, pp. 795–800.

[20] G. Tartarisco, N. Carbonaro, A. Tonacci, G. Bernava, A. Arnao, G. Crifaci, P. Cipresso, G. Riva, A. Gaggioli, D. De Rossi *et al.*, "Neuro-fuzzy physiological computing to assess stress levels in virtual reality therapy," *Interacting with Computers*, vol. 27, no. 5, pp. 521–533, 2015.

[21] N. Hjortskov, D. Rissén, A. K. Blangsted, N. Fallentin, U. Lundberg, and K. Søgaard, "The effect of mental stress on heart rate variability and blood pressure during computer work," *European journal of applied physiology*, vol. 92, no. 1-2, pp. 84–89, 2004.

[22] E. S. Mezzacappa, R. M. Kelsey, E. S. Katkin, and R. P. Sloan, "Vagal rebound and recovery from psychological stress," *Psychosomatic medicine*, vol. 63, no. 4, pp. 650–657, 2001.

[23] R. M. Stern, W. J. Ray, and K. S. Quigley, *Psychophysiological recording*. Oxford University Press, USA, 2001.

[24] L. Bernardi, J. Wdowczyk-Szulc, C. Valenti, S. Castoldi, C. Passino, G. Spadacini, and P. Sleight, "Effects of controlled breathing, mental activity and mental stress with or without verbalization on heart rate variability," *Journal of the American College of Cardiology*, vol. 35, no. 6, pp. 1462–1469, 2000.

[25] Y. Kuriyagawa and I. Kageyama, "A modeling of heart rate variability to estimate mental work load," in *Systems, Man, and Cybernetics, 1999. IEEE SMC'99 Conference Proceedings. 1999 IEEE International Conference on*, vol. 2. IEEE, 1999, pp. 294–299.

[26] D. W. Watson, "Physiological correlates of heart rate variability (hrv) and the subjective assessment of workload and fatigue in-flight crew: a practical study," in *Human Interfaces in Control Rooms, Cockpits and Command Centres, 2001. People in Control. The Second International Conference on (IEE Conf. Publ. No. 481)*. IET, 2001, pp. 159–163.

[27] R. Zheng, S. Yamabe, K. Nakano, and Y. Suda, "Biosignal analysis to assess mental stress in automatic driving of trucks: Palmar perspiration and masseter electromyography," *Sensors*, vol. 15, no. 3, pp. 5136–5150, 2015.

[28] H. Gao, A. Yüce, and J.-P. Thiran, "Detecting emotional stress from facial expressions for driving safety," in *Image Processing (ICIP), 2014 IEEE International Conference on*. IEEE, 2014, pp. 5961–5965.

[29] L. Torres-Salomao, M. Mahfouf, and E. El-Samahy, "Pupil diameter size marker for incremental mental stress detection," in *E-health Networking, Application & Services (HealthCom), 2015 17th International Conference on*. IEEE, 2015, pp. 286–291.

[30] C. He, M. Mahfouf, and L. A. Torres-Salomao, "Facial temperature markers for mental stress assessment in human-machine interface (hmi) control system," in *ICINCO*, 2018.

[31] S. Akselrod, D. Gordon, F. A. Ubel, D. C. Shannon, A. C. Barger, and R. J. Cohen, "Power spectrum analysis of heart rate fluctuation: a quantitative probe of beat-to-beat cardiovascular control," *science*, pp. 220–222, 1981.

[32] M. E. Smith, A. Gevins, H. Brown, A. Karnik, and R. Du, "Monitoring task loading with multivariate eeg measures during complex forms of human-computer interaction," *Human Factors*, vol. 43, no. 3, pp. 366–380, 2001.

[33] J. Chen, B. Hu, P. Moore, X. Zhang, and X. Ma, "Electroencephalogram-based emotion assessment system using ontology and data mining techniques," *Applied Soft Computing*, vol. 30, pp. 663–674, 2015.

[34] P. Ren, A. Barreto, Y. Gao, and M. Adjouadi, "Affective assessment of computer users based on processing the pupil diameter signal," in *Engineering in Medicine and Biology Society, EMBC, 2011 Annual International Conference of the IEEE*. IEEE, 2011, pp. 2594–2597.

[35] D. Kahneman, *Thinking, fast and slow*. Macmillan, 2011.

[36] G. L. Brengelmann, "Body surface temperature: Manifestation of complex anatomy and physiology of the cutaneous vasculature," in *Engineering in Medicine and Biology Society, 2000. Proceedings of the 22nd Annual International Conference of the IEEE*, vol. 3. IEEE, 2000, pp. 1927–1930.

[37] N. Charkoudian, "Skin blood flow in adult human thermoregulation: how it works, when it does not, and why," in *Mayo Clinic Proceedings*, vol. 78, no. 5. Elsevier, 2003, pp. 603–612.

[38] F. Chao, D. Zhou, C.-M. Lin, L. Yang, C. Zhou, and C. Shang, "Type-2 fuzzy hybrid controller network for robotic systems," *IEEE transactions on cybernetics*, 2019.

[39] J. M. Mendel, "A comparison of three approaches for estimating (synthesizing) an interval type-2 fuzzy set model of a linguistic term for computing with words," *Granular Computing*, vol. 1, no. 1, pp. 59–69, 2016.

[40] ——, *Uncertain rule-based fuzzy logic systems: introduction and new directions*. Prentice Hall PTR Upper Saddle River, 2001.

[41] H. Li, J. Wang, L. Wu, H.-K. Lam, and Y. Gao, "Optimal guaranteed cost sliding-mode control of interval type-2 fuzzy time-delay systems," *IEEE Transactions on Fuzzy Systems*, vol. 26, no. 1, pp. 246–257, 2017.

[42] M. C. Kennedy and A. O'Hagan, "Bayesian calibration of computer models," *Journal of the Royal Statistical Society: Series B (Statistical Methodology)*, vol. 63, no. 3, pp. 425–464, 2001.

Changjiang He received his MEng degree from the University of Sheffield, Sheffield, U.K., in 2015. He is currently in the last year of his PhD studies at the Department of Automatic Control and Systems Engineering of the University of Sheffield. His research interests include fuzzy logic modelling, psychophysiology, intelligent control systems and bioengineering.

Mahdi Mahfouf received his MPhil and PhD degrees from the University of Sheffield, Sheffield, U.K., in 1987 and 1991, respectively. He has been a personal chair in Intelligent Systems Engineering at the University of Sheffield since 2005. Professor Mahfouf is the author of more than 300 papers and has authored/coauthored one book and five book chapters. He has been working in the areas of intelligent systems modelling, optimisation and control in biomedicine as well as industrial systems for more than 30 years.

Luis A. Torres-Salomao received his PhD degree from the University of Sheffield, Sheffield, U.K., in 2016. His research interests include intelligent systems, nonlinear modelling and control in different disciplines (aviation, supply chain, fault detection, wind power, mental stress detection).